Hubble Tension and Gravitational Self-Interaction

Corey Sargent,¹ Alexandre Deur,^{2,1} and Balša Terzić¹

¹Department of Physics, Old Dominion University, Norfolk, Virginia 23529, USA

²Department of Physics, University of Virginia, Charlottesville, Virginia 22901, USA

One of the most important problems vexing the Λ CDM cosmological model is the Hubble tension. It arises from the fact that measurements of the present value of the Hubble parameter performed with low-redshift quantities, e.g., the Type IA supernova, tend to yield larger values than measurements from quantities originating at high-redshift, e.g., fits of cosmic microwave background radiation. It is becoming likely that the discrepancy, currently standing at 5σ , is not due to systematic errors in the measurements. Here we explore whether the self-interaction of gravitational fields in General Relativity, which are traditionally neglected when studying the evolution of the universe, can explain the tension. We find that with field self-interaction accounted for, both low- and high-redshift data are *simultaneously* well-fitted, thereby showing that gravitational self-interaction could explain the Hubble tension. Crucially, this is achieved without introducing additional parameters.

I. THE HUBBLE TENSION

Modern cosmology began with the discovery of Hubble's law. Its central element, the present value of the Hubble parameter, H_0 , has a troubled history of measurements and it is only in the last two decades since precise determinations became available. However, two types of precision measurements of H_0 are in conflict. The first type comprises observations of phenomena originating at high redshift z, principally the power spectrum of the cosmic microwave background (CMB) [1] and the baryon acoustic oscillations (BAO) [2]. The second type consists of determination of H_0 from low-z phenomena, notably using standard candles [3] and time-delay cosmography [4] methods. See [5] for the low- and high-z methods providing H_0 . The high-z phenomena yield H_0 values significantly lower than those from low-z. This is known as the "Hubble tension" [5–7]. The discrepancy presently reaches a 5σ significance: the combined high-z measurements yield 67.28 ± 0.60 km/s/Mpc while the combined low-z measurements yield $H_0 = 73.04 \pm 1.04$ km/s/Mpc [8]. Yet, individual low-z measurements can be as much as 6σ away [5] from the most precise high-z datum, the Planck satellite result [1].

Although the Hubble tension may originate from unaccounted systematic effects [9], the consistency of the high-z results on the one hand, and that of the low-z results on the other, suggests that it could instead reveal a limitation of the current standard model of cosmology, the dark energy-cold dark matter model (ACDM). This would be just one of the several malaises of ACDM. A first worry is that detection of dark matter particles by direct [10] or indirect [11] measurements is still wanting, with searches having almost exhausted the allowed parameter spaces of likely candidates. Furthermore, the most natural extensions of the standard model of particle physics which offer convincing dark matter candidates are mostly ruled out, e.g., minimal SUSY [12]. Other worries with ΛCDM include overestimating the number of globular clusters and dwarf galaxies [13] or the lack of uncontrived explanation for tight correlations between the supposedly sub-dominant baryonic matter and quantities characterizing galaxy dynamics, e.g., the Tully-Fisher relation [14], radial acceleration relation (RAR) [15], or Renzo's rule [16]. These issues motivate developing alternatives to Λ CDM that could naturally resolve these problems. Here we follow this direction and investigate whether the Hubble tension can be understood with a model that incorporates the fact that in General Relativity (GR), gravitational fields interact with each others (field self-interaction, SI). That central feature of GR is the basis for the GR-SI model. This model already explains the chief observations involving dark matter/energy without recourse to dark components: the flat rotation curves of galaxies [17, 18]; the high-z supernova luminosities [19]; the CMB anisotropies [20]; the formation of large structures [21]; the matter power spectrum [20]; the internal dynamics of galaxy clusters, including that of the Bullet Cluster [17]; and the RAR [22] and Tully-Fisher [17] relations.

In the next section, we recall the physical basis of the GR-SI framework and its predictions. We then discuss how, from the perspective of the GR-SI model, a Hubble tension should arise if low- and high-z data are analyzed with Λ CDM, and why the tension is not present in GR-SI. After summarizing how the evolution of the universe affects the CMB anisotropy observations in both the GR-SI and Λ CDM frameworks, we use GR-SI to fit luminosity distance data. This constrains the GR-SI parameters describing the effects of large-scale structure formation on the long distance propagation of gravity, effects that are encapsulated in a so-called depletion function $D_M(z)$. Finally, we verify that with the constrained parameters, the GR-SI fit reproduces better the CMB power spectrum with the low-z value of H_0 than with the high-z H_0 determination. We also find that if H_0 is left a free parameter, its best fit value agrees with the low-z determination rather than the high-z one. This indicates an absence of Hubble tension in the GR-SI model. We will consider only the scalar multipole coefficient $C_{TT,l}^s$ since it is sufficient to investigate

whether a Hubble tension is present in the GR-SI model. In particular, it is not necessary for the goal of this article to investigate the polarized CMB data.

II. FIELD SELF-INTERACTION AND ITS CONSEQUENCES

A defining feature of GR is that it is a non-linear theory: gravity fields interact with each other, in contrast to Newtonian gravity. The linear character of the latter allows for the field superposition principle, while in GR, the combination of fields differ from their sum since the fields interact. In fact, the GR Lagrangian $\mathcal{L}_{GR} = \sqrt{\det(g_{\mu\nu})} g_{\mu\nu} R^{\mu\nu}/(16\pi G)$ (here $g_{\mu\nu}$ is the metric, G is Newton's constant and $R_{\mu\nu}$ is the Ricci tensor) expressed in a polynomial form [23]:

$$\mathcal{L}_{GR} = \sum_{n=0}^{\infty} (16\pi MG)^{n/2} \left[\phi^n \partial \phi \partial \phi \right], \tag{1}$$

explicitly shows that a gravitational field self-interacts. Here, $\phi_{\mu\nu}$ is the gravitational field due to a unit mass and is defined as the deviation of $g_{\mu\nu}$ from a reference constant metric $\eta_{\mu\nu}$, $\phi_{\mu\nu} \equiv (g_{\mu\nu} - \eta_{\mu\nu})/\sqrt{M}$, where M is the mass of the system. For simplicity, we ignored the matter term of \mathcal{L}_{GR} : to discuss the pure field case is sufficient. The bracket in $[\phi^n \partial \phi \partial \phi]$ signifies a sum of Lorentz-invariant terms whose forms are $\phi^n \partial \phi \partial \phi$, e.g., $[\partial \phi \partial \phi]$ is the Fierz-Pauli Lagrangian of linearized GR [24]. Newtonian gravity is recovered if $\eta_{\mu\nu}$ is the Minkowski metric and if one keeps only the time-time component of the n=0 term of Eq. (1): $[\partial\phi\partial\phi]\partial^{\mu}\phi_{00}\partial_{\mu}\phi^{00}$ and $\partial^{0}\phi_{00}=0$. The term $[\partial\phi\partial\phi]$ formalizes the free motion of the field, viz, it generates the two-point correlation function that gives the probability for the field to freely propagate from one spacetime point to another. The n > 0 terms are interaction terms and therefore cause the field SI. An analogous phenomenon occurs for the nuclear Strong Force, whose theory is Quantum Chromodynamics (QCD). Actually, the reason why GR and QCD are non-linear theories is the same: they possess several types of distinct "charges". For GR, they are the mass/energy, momentum and stress. For QCD, they are the three color charges. This causes the fields of GR and QCD to be rank-2 tensors, i.e., non-commuting objects. The non-zero commutators in turn give rise to SI terms. It results in GR and QCD having the same Lagrangian structure. Field SI is a central and conspicuous feature of QCD due to its large coupling α_s [25]. In contrast, field SI in GR is controlled by $\sim \sqrt{GM/L}$ (with L a characteristic length of the system), whose value is typically small. This makes the linear approximations of GR, e.g., the Newtonian or the Fierz-Pauli theories, adequate for most applications. However, if $\sqrt{GM/L}$ is large enough, SI must be accounted for: it is an unavoidable consequence of GR. The calculations in [17, 18, 28] indicate that for galaxies or galaxy clusters, $\sqrt{GM/L}$ is large enough to enable SI.

One consequence of SI in QCD is to enhance the binding of quarks, resulting in their confinement. Likewise in GR, if a galactic mass is large enough to enable SI, it would enhance the binding of galactic components in a manner that directly leads to flat galactic rotation curves [17] without requiring dark matter. The increased binding also dispenses with the need for dark matter to account for the growth of large-scale structures [21]. On the other hand, using Newtonian gravity to analyze systems in which SI is important overlooks the binding enhancement and produces an apparent mass discrepancy interpreted as dark matter. Importantly, SI effects cancel out in isotropic and homogeneous systems. For example, a nearly spherical galaxy has much less evidence of dark matter than a flatter galaxy [26, 27].

Another direct and crucial consequence of the binding enhancement comes from energy conservation: the increase of binding energy inside a system must be balanced by a reduction of the gravitational energy outside of the system. In QCD, the larger binding confines quarks into hadrons, while outside hadrons, the Strong Force declines into the much weaker residual Yukawa interaction. Likewise, if SI binds more tightly massive systems, gravitation must be reduced outside these systems. Overlooking that large-distance reduction of gravity would require a compensating global repulsion in much the same way as overlooking the binding enhancement requires a compensating dark mass. The purported repulsion would then be interpreted as dark energy.

The enhanced binding of structures, viz, the local effect of SI, is computed starting from GR's Lagrangian, Eq. (1) [17, 28]. The large-distance suppression of gravity, viz, the global effect, is evaluated effectively using a depletion function $D_M(z)$ that originates from lifting the traditional assumptions that the universe is isotropic and homogeneous [19].

If $D_M = 0$, gravity is fully quenched at large-distance while for $D_M = 1$ there is no net SI effect. Thus, $D_M(z) \approx 1$ for the early universe since it was nearly isotropic and homogeneous. In contrast, the large-scale structures of the present universe entail $D_M(z \approx 0) < 1$. The form of $D_M(z)$ first proposed in [19] can be approximated by:

$$D_M(z) = 1 - (1 + e^{(z-z_0)/\tau})^{-1} + Ae^{-z/b}.$$
 (2)

Here, z_0 is the redshift characterizing the large-scale structure formation epoch and τ its duration. A is the mass fraction of structures whose shapes have evolved into more symmetric ones (e.g., disk galaxies merging to form elliptical galaxies) and b is the duration of that evolution process. Fig. 1 displays $D_M(z)$.

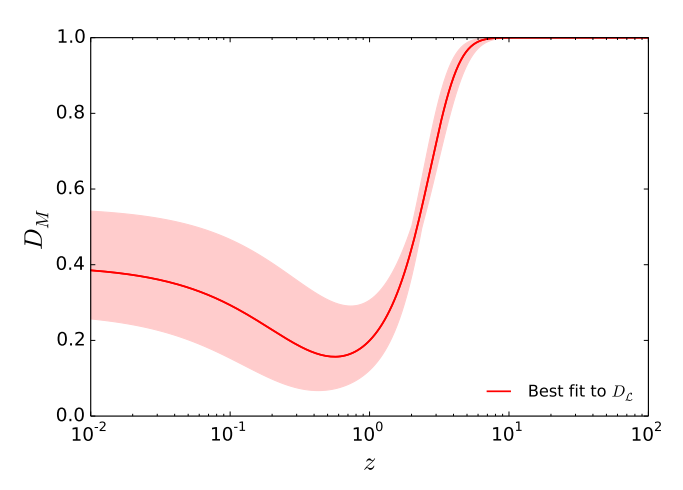


FIG. 1: Depletion function $D_M(z)$ determined from the optimizing the fit to the low- and high-z $D_{\mathcal{L}}$ data in Fig. 2.

III. THE HUBBLE TENSION FROM THE GR-SI PERSPECTIVE

A Hubble tension arising within Λ CDM is expected from the perspective of GR-SI: H_0 affects the observation of the CMB anisotropies essentially via the angular diameter distance of last scattering, d_A . This quantity depends upon the evolution of the universe similarly to the luminosity distance $D_{\mathcal{L}}$ that enters the lower-z determination of H_0 , e.g., via supernova observations. Specifically, $d_A(z) = D_{\mathcal{L}}(z)/(1+z)^2$. For example, in the Λ CDM model,

$$d_A(z) = \frac{1}{H_0(1+z)\sqrt{\Omega_K}} \sinh\left(\sqrt{\Omega_K} \int_{(1+z)^{-1}}^1 \frac{dx}{\sqrt{\Omega_\Lambda x^4 + \Omega_K x^2 + \Omega_M x + \Omega_\gamma}}\right),\tag{3}$$

$$D_{\mathcal{L}}(z) = \frac{(1+z)}{H_0 \sqrt{\Omega_K}} \sinh\left(\sqrt{\Omega_K} \int_{(1+z)^{-1}}^1 \frac{dx}{\sqrt{\Omega_\Lambda x^4 + \Omega_K x^2 + \Omega_M x + \Omega_\gamma}}\right),\tag{4}$$

with Ω_{Λ} , Ω_{M} and Ω_{γ} the dark energy, total matter and radiation densities relative to the critical density, respectively, and $\Omega_{K} \equiv {}^{K}/a_{0}^{2}H_{0}^{2}$ with K the curvature and a_{0} the Friedmann-Lemaître-Robertson-Walker scale factor at present time. Therefore, the determination of H_{0} from CMB observations is analogous to a highly accurate $D_{\mathcal{L}}(z_{L})$ observation, where z_{L} is the redshift at the time of last rescattering.

Figure 2 depicts two luminosity distances $D_{\mathcal{L}}(z)$ calculated within ΛCDM with $\Omega_{\Lambda} = 0.69$, $\Omega_{M} = 0.31$ and K = 0, but different H_{0} values: 73.06 km/s/Mpc, which matches the supernova and γ -ray data at low-z (dashed blue line in the left panel and blue dots in the right), and the other with 67.28 km/s/Mpc to match the CMB $D_{\mathcal{L}}(z_{L})$ (dotted green line and green points). The uncertainty of the CMB datum is adjusted to equalize the χ^{2}/ndf values of the fits for the comparison of the data and the two ΛCDM cosmologies. The Hubble tension is evident in the two ΛCDM curves which match well either the low-z data or the high-z data, but not both. However, the GR-SI model for $D_{\mathcal{L}}(z)$ [19],

$$D_{\mathcal{L}}(z) = \frac{(1+z)}{\sqrt{\Omega_K} H_0} \sinh\left(\sqrt{\Omega_K} \int_{1/(1+z_L)}^1 \frac{dx}{\sqrt{\Omega_K x^2 + D_M(1/x - 1)x}}\right),\tag{5}$$

fits both data sets well, as quantified by a significantly smaller χ^2/ndf value, therefore exhibiting no signs of Hubble tension. Here, we elected to let the parameters of $D_M(z)$ be determined from the best fit to the $D_{\mathcal{L}}(z)$ data. This yields $z_0 = 2.20 \pm 0.18$, $\tau = 0.84^{+0.15}_{-0.19}$, $A = 0.33 \pm 0.09$ and $b = 0.24^{+0.10}_{-0.16}$. Originally the values of the parameters were obtained from the knowledge of the evolution of large-scale structures. The value $z_0 = 2.20 \pm 0.18$ is smaller than the estimate from large structure formation, $z_0 = 6.3^{+1.6}_{-2.0}$ [21], but the ratio $z_0/\tau = 2.62$ happens to be the same for the fit and the estimates from large structure formation. The fit values for the A and b parameters agree with the earlier values, $A = 0.25^{+0.20}_{-0.17}$ and $b = 0.20^{+0.15}_{-0.05}$.

The $D_{\mathcal{L}}(z)$ calculated within Λ CDM and GR-SI differ chiefly at intermediate values of z because SI induces a large-distance suppression of gravity which curves $D_{\mathcal{L}}(z)$ in the $1 \lesssim z \lesssim 10$ domain, when large-scale structures start forming [19, 20].

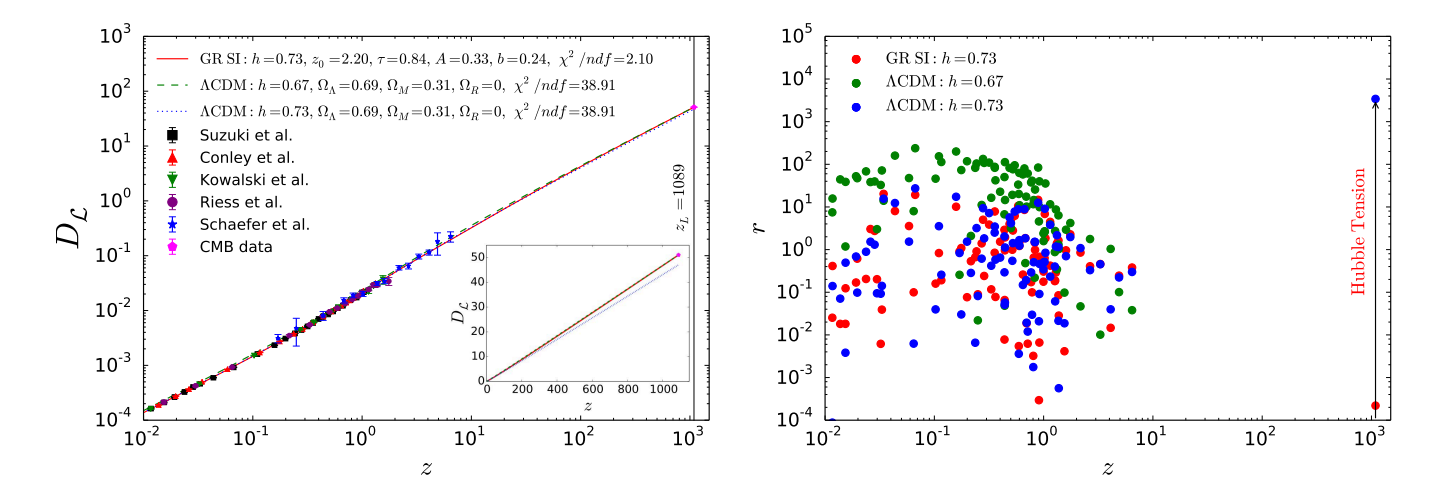


FIG. 2: Left: Luminosity distance $D_{\mathcal{L}}$ as a function of redshift z for: ΛCDM using $h \equiv ^{H_0/100 \text{ km/s/Mpc}} = 0.67$ (dashed green line) or h = 0.73 (dotted blue line); and GR-SI with h = 0.73 (solid red line). The embedded figure is the same but in linear rather than log scales. The low-z observational data, shown by the square, triangle, circle and star symbols, are normalized using the h = 0.73 average low-z determination. The pentagon symbol shows $D_{\mathcal{L}}(z_L)$ as it would be obtained using the values of z_L and H_0 from the ΛCDM fit of the CMB. Right: Same as the left panel but for the normalized residual $r = (D_{\mathcal{L}} - d_{\text{obs}})^2/e_{\text{obs}}^2$, where d_{obs} is the observed data, e_{obs} their uncertainty, and the colors match that of the three different models used to compute $D_{\mathcal{L}}$ in the left panel. The Hubble tension appears as the offset between the ΛCDM curve which fits the low-z data (dotted blue line in the left panel and blue dots in the right panel) and the blue dot at z_L . The green dot at z_L is near r = 0 and hence not visible with the log scale.

The specific timing and amount of matter involved in the formation of large-scale structures result in the particular z-dependence of $D_M(z)$ which differs from the $\propto z^4$ effect of dark energy in Λ CDM. Thus, if SI noticeably influences the evolution of the universe, there will arise a discrepancy with $D_{\mathcal{L}}(z)$ determinations using smaller-z phenomena for which the evolution spans a much smaller range. Since the determination of H_0 from the CMB is analogous to a determination using $D_{\mathcal{L}}(z_L)$, extracting H_0 from the CMB using the Λ CDM framework will cause a tension with H_0 measurements at lower z. The same applies to the baryonic acoustic oscillations (BAO) observation from the CMB. It is characterized by the acoustic horizon angular size, $\theta = {}^{d_H}/{}^{d_A(z_L)}$, where d_H is the acoustic horizon. Since d_H is the comoving distance travelled by a sound wave until recombination, viz, it happens for $z > z_L$ when the universe was homogeneous and dark energy negligible, d_H is essentially the same for Λ CDM and GR-SI. It is the distinct evolution of $d_A(z)$ in Λ CDM and GR-SI that makes their θ predictions different. Like $D_{\mathcal{L}}$, d_A is predicted by Λ CDM to be larger at z = 0, yielding smaller θ and H_0 values compared to local measurements and the expectation from GR-SI.

IV. DEPENDENCE OF THE CMB OBSERVATIONS ON THE EXPANSION OF THE UNIVERSE

The GR-SI fit of $D_{\mathcal{L}}(z)$ just discussed indicates that there is no Hubble tension in the GR-SI model. An independent test that would support this conclusion is to fit the CMB within the GR-SI framework, and check that the low-z H_0 determination provides a better fit to the CMB than the high-z H_0 one. We use an analytical expression of the CMB anisotropies to show how the expansion of the universe affects their observations at present-day. Such analytical expression is provided by the hydrodynamic approximation [29]. Despite not being as accurate as state-of-the-art numerical treatments of the CMB, this treatment is sufficient for the goal of this article, namely to investigate the Hubble tension within the GR-SI model. This is verified a posteriori by the small χ^2/ndf characterizing the GR-SI fits to the CMB. At z_L , the universe is very homogeneous, making SI effects negligible. Thus, the phenomena that created the CMB anisotropies are unaffected and so are the mathematical expressions formalizing them. However, some of the parameters entering the CMB anisotropy expression use their present time values. They are thus affected by the expansion of the universe and therefore contribute to the Hubble tension. In what follows, values of parameters at the present time, matter-radiation equilibrium time, and last scattering time are indicated by the subscripts 0, EQ and L, respectively. Baryon relative density is denoted by Ω_B , and, for Λ CDM, the dark matter relative density is Ω_{DM} . We consider $C_{TT,l}^s$, the scalar multipole coefficient for the temperature-temperature angular correlation (here

TABLE I: CMB quantities depending explicitly on the expansion of the universe. Column 1: quantity. Column 2: Λ CDM expression. Column 3: GR-SI expression.

	ΛCDM	GR-SI
d_A	$\frac{1}{\sqrt{\Omega_K}H_0(1+z_L)}\sinh\left(\sqrt{\Omega_K}\int_{1/(1+z_L)}^1\frac{dx}{\sqrt{\Omega_\Lambda x^4+\Omega_K x^2+\Omega_M x}}\right)$	$ \frac{1}{\sqrt{\Omega_K} H_0(1+z_L)} \sinh \left(\sqrt{\Omega_K} \int_{1/(1+z_L)}^1 \frac{dx}{\sqrt{\Omega_K x^2 + D_M(1/x - 1)x}} \right) $
t_L	$\frac{1}{H_0} \int_0^{1/(1+z_L)} \frac{xdx}{\sqrt{\Omega_\Lambda x^4 + \Omega_K x^2 + \Omega_M x + \Omega_R}}$	$\frac{1}{H_0} \int_0^{1/(1+z_L)} \frac{x dx}{\sqrt{\Omega_K x^2 + D_M (1/x - 1) + \Omega_R}}$

l is the multipole moment). Its expression within the hydrodynamic approximation is provided in [29]:

$$\frac{l(l+1)C_{TT,l}^{s}}{2\pi} = \frac{4\pi T_{0}^{2}N^{2}e^{-2\tau_{reion}}}{25} \int_{1}^{\infty} d\beta \left(\frac{\beta l}{l_{\mathcal{R}}}\right)^{n_{s}-1} \left\{ \frac{3\sqrt{\beta^{2}-1}}{\beta^{4}(1+R_{L})^{3/2}} \mathcal{S}^{2}(\beta l/l_{T})e^{-2\beta^{2}l^{2}/l_{D}^{2}} \sin^{2}\left(\beta l/l_{H} + \Delta(\beta l/l_{T})\right) + \frac{1}{\beta^{2}\sqrt{\beta^{2}-1}} \left[3\mathcal{T}(\beta l/l_{T})R_{L} - (1+R_{L})^{-1/4}\mathcal{S}(\beta l/l_{T})e^{-\beta^{2}l^{2}/l_{D}^{2}} \cos\left(\beta l/l_{H} + \Delta(\beta l/l_{T})\right) \right]^{2} \right\} + \mathcal{C}(l). \quad (6)$$

The first term in the curly bracket formalizes the Doppler effect. The second term provides the Sachs-Wolf and intrinsic temperature anisotropy effects. Both terms also contains the large-l damping. N is the normalization of the primordial perturbations, τ_{reion} is the reionized plasma optical depth, β is an integration variable akin to a wave number, n_s is the scalar spectral index, $l_R \equiv (1+z_L)k_R d_A$ is a multipole characteristic value, with $k_R \equiv 0.05 \; \mathrm{Mpc}^{-1}$ a conventional scale. Other multipole characteristic values are $l_T = d_A/d_T$ (d_T is a length scale whose form differs in $\Lambda \mathrm{CDM}$ and GR-SI; see below), $l_D = d_A/d_D$ (d_D is the damping length) and $l_H = d_A/d_H$. $R_L = {3\Omega_B}/{4\Omega_{\gamma}(1+z_L)}$ is a ratio of relative densities and \mathcal{S} , \mathcal{T} and Δ are transfer functions. Finally, $\mathcal{C}(l)$ is a second-order term correcting the approximations of the hydrodynamic model [20]. Hereafter, since $\mathcal{C}(l)$ is small, we will ignore its possible dependence on the difference between the universe evolutions according to $\Lambda \mathrm{CDM}$ and GR-SI. The integrated Sachs-Wolf, Sunyaev-Zel'dovich and cosmic variance effects, which produce anisotropies that are extrinsic to the CMB origin, are not included in the hydrodynamic model. This does not affect our study of the Hubble tension since we will focus on the multipole range 48 < l < 1800, a domain where these effects are unimportant.

In Eq. (6), the quantities that depend on the expansion of the universe are integrated over z. There are only two such parameters: d_A and t_L . Their expressions in Λ CDM and GR-SI are given in Table I. The expressions of the quantities not explicitly affected by the expansion of the universe are tabulated in Appendix for convenience. Some of these quantities depend indirectly on the expansion of the universe as they contain t_L , z_L or d_A , namely d_T , R_L , d_{Landau} , d_{Silk} , d_H and d_D (the latter through d_{Landau} and d_{Silk}), l_R , l_T , l_D and l_H . In all, this shows that the Hubble tension may be cast as the problem of properly modeling the distances d_A and $D_{\mathcal{L}}$. In fact, once SI is accounted for in the CMB anisotropy expression, we can fit the $C_{TT,l}^s$ data while keeping H_0 to its low-z determination of 73.06 km/s/Mpc and the $D_M(z)$ parameters obtained from the best fit of $D_{\mathcal{L}}(z)$ (red line of Fig. 1). The parameters allowed to vary are z_L , N, n_s , σ and Ω_B , with the $C^s_{TT,l}$ spectrum reproduced for $z_L = 1728 \pm 1, \ N = (1.1995 \pm 0.0019) \times 10^{-5}, \ n_s = 0.9759 \pm 0.0028, \ \sigma = 1.751 \pm 0.0002 \ \text{and} \ \Omega_B h^2 = 0.370 \pm 0.002,$ with $\chi^2/ndf = 0.59$, see Fig. 3. We remark that the quoted uncertainties are only fit uncertainties and do not include other systematic effects, e.g., coming from approximations in the CMB hydrodynamics model or from the choice of functional form for $D_M(z)$ and its parameters. This fit must use the H_0 value determined by low-z observations since there is no Hubble tension in the GR-SI model due to the universe expanding differently than in the ΛCDM model. This is verified by performing a CMB fit with $H_0 = 67.28 \text{ km/s/Mpc}$ and observing that the χ^2/ndf of that fit is larger (by about 20%) than that of the nominal fit. It is also interesting to perform the fit with H_0 kept a free parameter despite the fact that it introduces a slight inconsistency since the determination of the $D_M(z)$ parameters is obtained with the H_0 value fixed by $z \simeq 0$ observations. Such fit yields $H_0 = 72.99 \pm 0.06$ km/s/Mpc, $z_L = 1728 \pm 1$, $N = (1.2014 \pm 0.0015) \times 10^{-5}$, $n_s = 0.9738 \pm 0.0027$, $\sigma = 1.751 \pm 0.002$ and $\Omega_B h^2 = 0.368 \pm 0.002$, with $\chi^2/ndf = 0.58$.

V. CONCLUSION

Our results show that the Hubble tension may be resolved if one accounts, when quantifying the evolution of the universe, for the self-interaction of gravitational fields, a feature of General Relativity ordinarily neglected. In the cosmological model used in this article, as in the previous studies using that model, the effects of self-interaction are contained within a depletion function which effectively relaxes the traditional assumptions of the Cosmological Principle—isotropy and homogeneity of the evolving universe. Here, the parameters of the depletion function are

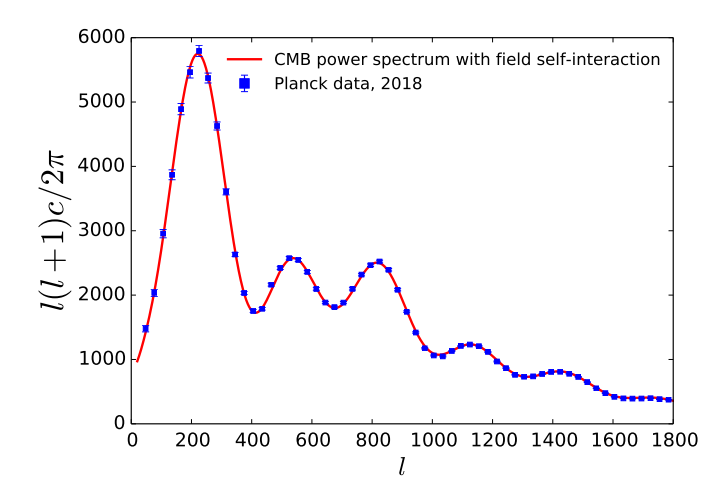


FIG. 3: Power spectrum of the CMB temperature anisotropy. The continuous line is $l(l+1)C_{TT,l}^{s}/(2\pi)$ computed using GR-SI with the low-z average for the Hubble parameter, $H_0 = 73.06$ km/s/Mpc. The squares are the Planck measurement ([30], 2018 release).

determined from the best fit to the luminosity distance data, a procedure that appears more accurate than the method used in [19], viz, determining the parameters from our knowledge of the timescale at which large-scale structures form, and of the amount of baryonic matter present in these structures. We show that the resulting luminosity distance fits simultaneously both low-redshift supernovae data as well as high-redshift CMB data. Furthermore, the model, with the depletion function thus determined, fits better the CMB power spectrum data with the H_0 value determined by the low-z observations, supporting the finding that there is no Hubble tension in the GR-SI model. Crucially, this possible solution to the problem of the Hubble tension does not require adding parameters beyond those already present in the model. This is important because to be compelling alternate to Λ CDM, a model should display a consistency and simplicity on par with Λ CDM, i.e., it should avoid introducing too many new and ad-hoc parameters, particles or fields. This is the case for the model used here which requires no new physics beyond the standard model of particle physics and General Relativity. Explaining the Hubble tension did not compromise this attractive feature of the model.

Acknowledgements

This work is done in part with the support of the U. S. National Science Foundation award No. 1847771. The authors are grateful to A. Mand and T. Möller for their useful comments on the manuscript.

TABLE II: Expressions of the quantities that are not explicitly dependent on the expansion of the universe. Column 1: Quantity. Column 2: Λ CDM expression. Column 3: GR-SI expression. In these expressions, σ is the standard deviation for the temperature T_L , $Y \simeq 0.24$ is the density ratio of nucleons to neutral ⁴He, σ_T is the Thompson cross-section, ρ_B and ρ_γ are average absolute densities of baryon and radiation, respectively, and n_{B0} is the baryon number density at present time.

	FLRW universe	Universe with GR's SI accounted for
d_T	$\sqrt{\Omega_R}/[(1+z_L)H_0\Omega_M]$	$\sqrt{\Omega_R}/[(1+z_L)H_0D_M(0)]$
R_L	$[3\Omega_B]/[4\Omega_{\gamma}(1+z_L)]$	Same as for Λ CDM
R_{EQ}	$[3\Omega_R\Omega_B]/[4\Omega_M\Omega_\gamma]$	$[3\Omega_R\Omega_B]/[4\Omega_MD(0)\Omega_{\gamma}]$
d_H	$\frac{2}{H_0(3R_L\Omega_M)^{1/2}(1+z_L)^{3/2}}\ln([\sqrt{1+R_L}+\sqrt{R_{EQ}+R_L}]/[1+\sqrt{R_{EQ}}])$	$\frac{2}{H_0(3R_LD_M(0))^{1/2}(1+z_L)^{3/2}}\ln([\sqrt{1+R_L}+\sqrt{R_{EQ}+R_L}]/[1+\sqrt{R_{EQ}}])$
d_D	$\sqrt{d_{ m Landau}^2 + d_{ m Silk}^2} = \sqrt{3\sigma^2 t_L^2}$	Same as for Λ CDM
$d^2_{ m Landau}$	$\frac{1}{8T_L^2(1+R_L)}$,	Same as for Λ CDM
d_{Silk}^2	$\left[\frac{R_L^2}{6(1-Y)(n_{B0})\sigma_T H_0\sqrt{\Omega_M}} R_0^{9/2} \int_0^{R_L} \frac{R^2 dR}{X(R)(1+R)\sqrt{R_{EQ}+R}} \left[\frac{16}{15} + \frac{R^2}{1+R}\right]\right]$	$\frac{R_L^2}{6(1-Y)(n_{B0})\sigma_T H_0 \sqrt{D_M(0)} R_0^{g/2}} \int_0^{R_L} \frac{R^2 dR}{X(R)(1+R) \sqrt{R_{EQ}+R}} \left[\frac{16}{15} + \frac{R^2}{1+R} \right]$ Same as for ACDM
R(t)	$-(\gamma/4p_{\gamma}(v))$	Same as for MCDW
X(T)	$1/\left[X^{-1}(3400) + \frac{\Omega_B h^2}{(\Omega_M h^2)^{1/2}} \int_T^{3400} g(T') dT'\right]$	$1/\left[X^{-1}(3400) + \frac{\Omega_B h^2}{(D_M(0)h^2)^{1/2}} \int_T^{3400} g(T')dT'\right]$

- N. Aghanim et al. [Planck], Astron. Astrophys. 641 (2020), A6 [erratum: Astron. Astrophys. 652 (2021), C4]
 [arXiv:1807.06209 [astro-ph.CO]].
- [2] S. Alam et al. [eBOSS], Phys. Rev. D 103 (2021) no.8, 083533 [arXiv:2007.08991 [astro-ph.CO]].
- [3] A. G. Riess, L. M. Macri, S. L. Hoffmann, D. Scolnic, S. Casertano, A. V. Filippenko, B. E. Tucker, M. J. Reid, D. O. Jones and J. M. Silverman, et al. Astrophys. J. 826 (2016) no.1, 56 [arXiv:1604.01424 [astro-ph.CO]].
- [4] K. C. Wong, S. H. Suyu, G. C. F. Chen, C. E. Rusu, M. Millon, D. Sluse, V. Bonvin, C. D. Fassnacht, S. Taubenberger and M. W. Auger, et al. Mon. Not. Roy. Astron. Soc. 498 (2020) no.1, 1420-1439 [arXiv:1907.04869 [astro-ph.CO]].
- [5] E. Abdalla, G. Franco Abellán, A. Aboubrahim, A. Agnello, O. Akarsu, Y. Akrami, G. Alestas, D. Aloni, L. Amendola and L. A. Anchordoqui, et al. JHEAp 34 (2022), 49-211 [arXiv:2203.06142 [astro-ph.CO]].
- [6] L. Verde, T. Treu and A. G. Riess, Nature Astron. 3, 891 [arXiv:1907.10625 [astro-ph.CO]].
- [7] E. Di Valentino, O. Mena, S. Pan, L. Visinelli, W. Yang, A. Melchiorri, D. F. Mota, A. G. Riess and J. Silk, Class. Quant. Grav. 38 (2021) no.15, 153001 [arXiv:2103.01183 [astro-ph.CO]].
- [8] A. G. Riess, W. Yuan, L. M. Macri, D. Scolnic, D. Brout, S. Casertano, D. O. Jones, Y. Murakami, L. Breuval and T. G. Brink, et al. Astrophys. J. Lett. 934 (2022) no.1, L7 [arXiv:2112.04510 [astro-ph.CO]].
- [9] W. L. Freedman, B. F. Madore, T. Hoyt, I. S. Jang, R. Beaton, M. G. Lee, A. Monson, J. Neeley and J. Rich, [arXiv:2002.01550 [astro-ph.GA]].
- [10] F. Kahlhoefer, Int. J. Mod. Phys. A 32 (2017) no.13, 1730006 [arXiv:1702.02430 [hep-ph]].
- J. M. Gaskins, Contemp. Phys. 57 (2016) no.4, 496-525 [arXiv:1604.00014 [astro-ph.HE]].
- [12] G. Arcadi, M. Dutra, P. Ghosh, M. Lindner, Y. Mambrini, M. Pierre, S. Profumo and F. S. Queiroz, Eur. Phys. J. C 78 (2018) no.3, 203 [arXiv:1703.07364 [hep-ph]].
- [13] A. A. Klypin, A. V. Kravtsov, O. Valenzuela and F. Prada, Astrophys. J. 522 (1999), 82-92 [arXiv:astro-ph/9901240 [astro-ph]].
- [14] R. B. Tully and J. R. Fisher, Astron. Astrophys. 54 (1977), 661-673
- [15] S. McGaugh, F. Lelli and J. Schombert, Phys. Rev. Lett. 117 (2016) no.20, 201101 [arXiv:1609.05917 [astro-ph.GA]].
- [16] R. Sancisi, IAU Symp. 220 (2004), 233 [arXiv:astro-ph/0311348 [astro-ph]].
- [17] A. Deur, Phys. Lett. B **676** (2009), 21-24 [arXiv:0901.4005 [astro-ph.CO]].
- [18] A. Deur, Eur. Phys. J. C 81 (2021) no.3, 213 [arXiv:2004.05905 [astro-ph.GA]].
- [19] A. Deur, Eur. Phys. J. C **79** (2019) no.10, 883 [arXiv:1709.02481 [astro-ph.CO]].
- [20] A. Deur, Class. Quant. Grav. 39 (2022) no.13, 135003 [arXiv:2203.02350 [gr-qc]].
- [21] A. Deur, Phys. Lett. B **820** (2021), 136510 [arXiv:2108.04649 [physics.gen-ph]].
- [22] A. Deur, C. Sargent and B. Terzić, Astrophys. J. 896 (2020) no.2, 94 [arXiv:1909.00095 [astro-ph.GA]].
- [23] A. Zee, Princeton University Press, 2013, ISBN 978-0-691-14558-7
- [24] M. Fierz and W. Pauli, Proc. Roy. Soc. Lond. A 173 (1939), 211-232
- [25] A. Deur, S. J. Brodsky and G. F. de Teramond, Nucl. Phys. 90 (2016), 1 [arXiv:1604.08082 [hep-ph]].
- [26] A. Deur, Mon. Not. Roy. Astron. Soc. 438 (2014) no.2, 1535-1551 [arXiv:1304.6932 [astro-ph.GA]].
- [27] D. Winters, A. Deur and X. Zheng, Mon. Not. Roy. Astron. Soc. 518 (2022) no.2, 2845-2852 [arXiv:2207.02945 [astro-ph.GA]].
- [28] A. Deur, Eur. Phys. J. C 77 (2017) no.6, 412 [arXiv:1611.05515 [hep-ph]].
- [29] S. Weinberg,
- [30] N. Aghanim et al. [Planck], Astron. Astrophys. 641 (2020), A5 [arXiv:1907.12875 [astro-ph.CO]].